

Magnetism in the layered transition-metal thiophosphates MPS_3 ($M = Mn, Fe, \text{ and } Ni$)

P. A. Joy and S. Vasudevan

Department of Inorganic and Physical Chemistry, Indian Institute of Science, Bangalore 560 012, India

(Received 22 January 1991; revised manuscript received 3 March 1992)

Anisotropic magnetic susceptibilities of single crystals of the layered transition-metal thiophosphates $MnPS_3$, $FePS_3$, and $NiPS_3$ have been measured as a function of temperature. The materials order antiferromagnetically at low temperatures, the Néel temperatures being 78, 123, and 155 K, respectively. In the ordered state, the magnetization axis lies perpendicular to the layers for $MnPS_3$ and $FePS_3$, while for $NiPS_3$ it lies in the layer. In the paramagnetic regime, the anisotropies of these compounds are different; while the susceptibility for $MnPS_3$ is isotropic and that for $NiPS_3$ shows only a weak anisotropy, $FePS_3$ exhibits highly anisotropic susceptibility. The anisotropic susceptibilities have been analyzed to obtain information on the state of the magnetic ions and the nature of magnetic interactions between them. The results show that $MnPS_3$, $FePS_3$, and $NiPS_3$ form a unique class of compounds. Although all three compounds are isostructural with the magnetic lattice being the two-dimensional honeycomb, the spin dimensionalities for the three are different. While $MnPS_3$ is best described by the isotropic Heisenberg Hamiltonian, $FePS_3$ is most effectively treated by the Ising model and $NiPS_3$ by the anisotropic Heisenberg Hamiltonian. The origin of the anisotropy in these compounds has been discussed, and it is shown how it arises from a combination of spin-orbit coupling and the trigonal distortion of the MS_6 octahedra. The magnetic exchange constant, J and the zero-field splitting energies of the ground state of the transition-metal ion have been evaluated from the anisotropic paramagnetic susceptibilities.

I. INTRODUCTION

Low-dimensional magnetic systems have gained special interest in the last two decades because of the variety of interesting phenomena that they exhibit. An important feature of this type of material is the short-range ordering of spins at temperatures higher than the critical temperature. There are numerous examples in the literature of low-dimensional magnetic systems.¹⁻³ In these systems the interaction of magnetic ions with their nearest neighbors is, in a particular spatial sense, mainly due to the typical structure of these compounds. Most of the known two-dimensional magnetic systems are not structurally two-dimensional. The magnetic layers in these compounds are separated by nonmagnetic groups. Well-known examples of this class of compounds are the K_2NiF_4 structure. This structure may be derived from the perovskite $KNiF_3$ lattice by the introduction of nonmagnetic KF sheets between the NiF_2 layers. Other examples are the copper chlorides of the general formula $(C_nH_{2n+1}NH_3)_2CuCl_4$ which are structurally and magnetically two-dimensional. The ferromagnetic layers of copper ions are separated by two layers of nonmagnetic alkylammonium groups. By increasing the value of n , the interlayer separation can be varied. Transition-metal dihalides also belong to this category. In all these compounds, the addition of nonmagnetic layers transforms the three-dimensional magnetic lattice to a magnetic layer structure. Some of the two-dimensional magnetic structures show interesting phenomena such as metamagnetism, canting, weak ferromagnetism, etc.

Layered transition-metal thiophosphates,⁴ MPS_3 , where M is a first-row transition metal, represents one of

the known layered systems in which both magnetic and crystallographic lattices are two-dimensional. Unlike the other two-dimensional magnetic systems, where the magnetic layers are separated by nonmagnetic layers, the MPS_3 layers are separated by a van der Waals gap. In this type of compound, superexchange pathways between the layers are ruled out due to the presence of a van der Waals gap. The interplanar $M-M$ distance is of the order of the third-neighbor $M-M$ distance within the same plane, so that direct exchange would be negligible and the magnetic interactions between the layers would be extremely weak. Hence these compounds may be viewed as "perfect" two-dimensional magnetic systems. Another example for this class of compounds is $FeOCl$.⁵

In this paper we report a detailed study of the magnetic susceptibilities of $MnPS_3$, $FePS_3$, and $NiPS_3$. Crystal structures of these compounds are well known⁶ and are related to the $CdCl_2$ structure. Sulphur atoms form a cubic close-packed array with the metal ions and P_2 pairs occupying the octahedral vacancies. The metal ions within a layer have a honeycomb arrangement and the MS_6 octahedra show a small trigonal distortion. The magnetic as well as the crystal layers in the transition-metal thiophosphates are separated by a van der Waals gap. All the three compounds are antiferromagnets with Néel temperatures 80, 123, and 155 K, respectively.⁷ The susceptibility in the paramagnetic region shows that the divalent transition-metal ions are in their high spin configuration. Magnetic structures for $MnPS_3$ and $FePS_3$ have been reported.⁸ The in-plane magnetic structures are shown in Fig. 1. It may be seen that although both are antiferromagnets, the type of ordering is quite different. For $MnPS_3$, all nearest-neighbor interactions

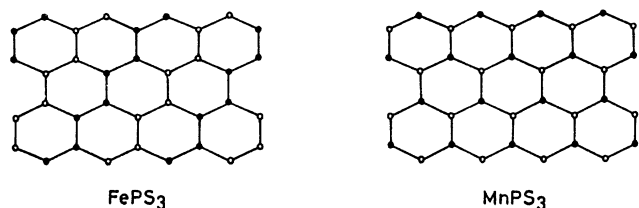


FIG. 1. The in-plane magnetic structures of MnPS_3 and FePS_3 .

within a layer are antiferromagnetic, whereas in FePS_3 , Fe^{2+} is coupled ferromagnetically to two of the nearest neighbors and antiferromagnetically to the third so that within the layer the Fe^{2+} moments appear as ferromagnetic chains coupled antiferromagnetically to each other. For both compounds the moments are perpendicular to the layer (parallel to the ab plane). The magnetic structure of NiPS_3 has been reported⁷ to be similar to that of FePS_3 . The only difference is that, for NiPS_3 , the magnetic and crystallographic unit cells are identical.

Since the transition-metal thiophosphate layers are separated by a van der Waals gap, they may be intercalated by a wide variety of guest molecules or ions^{4,9} similar to that reported for transition-metal dichalcogenides.¹⁰ Subsequent to intercalation the magnetic properties are considerably altered,¹¹ the reasons for which are as yet poorly understood. The present investigation arises from a need to understand in greater detail the nature of magnetic interactions in the pure host compounds, a prerequisite to the understanding of magnetism in the intercalated compounds. A detailed study of single-crystal anisotropic susceptibilities has been carried out for MnPS_3 , FePS_3 , and NiPS_3 and the data analyzed to obtain information on the state of the magnetic ions and the nature of magnetic interactions between them. The results show that MnPS_3 , FePS_3 , and NiPS_3 form a unique class of compounds. Although all three compounds are isostructural, with the magnetic lattice being the two-dimensional (2D) honeycomb, the spin dimensionalities of the three are different. While MnPS_3 is best described by the isotropic Heisenberg Hamiltonian, FePS_3 is most effectively treated by the Ising model, while NiPS_3 is best described by the anisotropic ($J_{\perp} > J_{\parallel}$) Heisenberg Hamiltonian. This paper discusses the origin of the anisotropy in these compounds and shows how it arises from purely crystal-field effects.

II. THEORETICAL BACKGROUND

In interpreting the magnetic data of the transition-metal thiophosphates, two points are of importance: first, the two-dimensional nature of magnetic interactions (both direct and super exchange) and second, the fact that the MS_6 octahedra are trigonally distorted, the trigonal axis being perpendicular to the layer. The trigonal distortion of the MS_6 octahedra has considerable importance on the type of magnetic behavior as well as the ordering. The effect of the trigonal distortion is to lift the

degeneracy of some of the states of the octahedral symmetry.

The effect of this distortion on the magnetic behavior is best considered in terms of the spin Hamiltonian. In the absence of any distortion, magnetic interactions between neighboring ions in the lattice may be treated by the Heisenberg Hamiltonian,

$$H = -2 \sum \{ J_{\perp} (S_{ix} S_{jx} + S_{iy} S_{jy}) + J_{\parallel} (S_{iz} S_{jz}) \}, \quad (1)$$

where the summation is over all pairs of magnetic ions in the lattice and the spins are treated as three-component vectors. In situations where $J_{\perp} = 0$, one has the Ising model and when $J_{\parallel} = 0$, one obtains the XY model. When $J_{\parallel} = J_{\perp}$ one obtains the isotropic Heisenberg Hamiltonian. The effect of axial distortion is to introduce an additional term, the single-ion anisotropy,

$$H = -2 \sum JS_i S_j + DS_{iz}^2. \quad (2)$$

The quadratic axial crystal-field parameter D arises from the combined effect of the crystal-field and spin-orbit splitting. The above form of the Hamiltonian is valid only in situations where the ground state is orbitally nondegenerate as with S state ions (e.g., Mn^{2+} or Fe^{3+}), or when the orbital angular momentum L is quenched by the crystal field (e.g., Cr^{3+} or Ni^{2+} in an octahedral field). In situations where the ground state is orbitally degenerate as in Fe^{2+} , a slightly different procedure has to be adopted and this is outlined in the next section.

The effect of D is to introduce anisotropy in the otherwise isotropic ($J_{\parallel} = J_{\perp}$) Heisenberg Hamiltonian. In situations where $D > J$, depending on the sign of D , the crystal field could establish a preference for the moments to align parallel or perpendicular to the z axis, corresponding to a planar- (XY) or axial- (Ising) type anisotropy. In the case when $D \ll J$ the isotropic Heisenberg Hamiltonian would be approached. This is probably the situation in the Mn^{2+} compounds. If the anisotropy is not fully uniaxial, an additional term $E(S_z^2 + S_y^2)$ would have to be added to Eq. (2) and the spin anisotropy will be orthorhombic. This, however, is not the situation in the transition-metal chalcogenophosphates.

It should be remembered, however, that the anisotropy in the Hamiltonian is not due to anisotropic exchange between isotropic moments but arises from the anisotropy in the expectation value of the spin moments. The transition-metal chalcogenophosphates are two-dimensional magnetic systems where the axial distortion of the MS_6 octahedra is likely to give rise to anisotropic terms which should dominate in determining the spin dimensionality (Ising, XY , or Heisenberg) of the compound. In these compounds the exchange would be mainly superexchange in origin. The sign and the nature of the superexchange interaction depend on the M - S - M angle as well as the d -electron occupancy of the metal ion and have been extensively documented in the literature¹² (Goodenough-Kanamori rules).

III. EXPERIMENTAL

MnPS₃, FePS₃ and NiPS₃ were synthesized from the corresponding elements and their single crystals were grown by the chemical vapor transport method.¹³ Magnetic-susceptibility measurements were made on a vibrating sample magnetometer (VSM) EG & G PAR model 155. Crystals of the sample were attached to the end of a wedge-shaped teflon piece. The temperature of the sample was varied from 55 to 300 K using a liquid-nitrogen glass Dewar. Temperatures below 78 K were attained by pumping on the liquid nitrogen. Measurements in the temperature range 300–675 K were performed using the high-temperature assembly supplied with the instrument. The susceptibility of the samples was obtained using Hg[Co(NCS)₄] as standard.

The output of the magnetometer and the temperature sensors (platinum resistance thermometer for low-temperature measurement and Cr-Al thermocouple in the high-temperature assembly) were fed into a computer through an IEEE-488 interface bus. Susceptibility was recorded continuously as a function of temperature. The susceptibilities reported here have been corrected for the diamagnetic contributions.

IV. RESULTS

A. MnPS₃

The temperature variation of the magnetic susceptibility of MnPS₃ is shown in Fig. 2. The susceptibility which is isotropic shows a broad maximum at 120 K. Below 100 K, χ_{\parallel} shows a sharp decrease with χ_{\perp} remaining essentially constant. The low-temperature behavior is typical of antiferromagnetic ordering, where the susceptibility parallel to the magnetization axis shows a sharp decrease below the Néel temperature, whereas the suscepti-

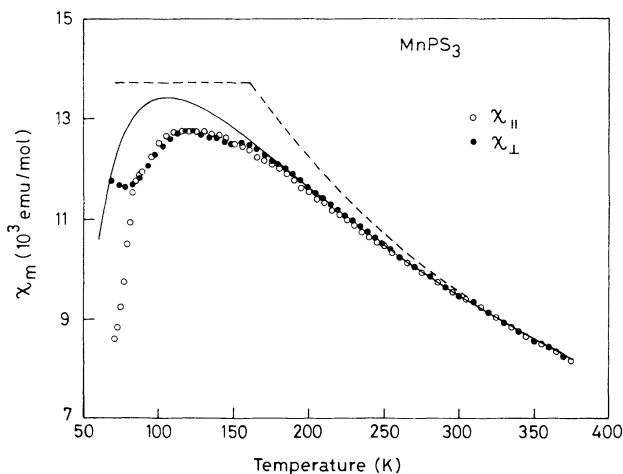


FIG. 2. Magnetic susceptibility of MnPS₃ single crystals, parallel (χ_{\parallel}) and perpendicular (χ_{\perp}) to the trigonal axis, as a function of temperature. The broken line and the solid line are the calculated susceptibility in the mean-field approximation [Eq. (14)] and high-temperature series expansion [Eq. (15)], respectively.

bility perpendicular to the axis remains constant (in the mean-field approximation). Figure 2 shows that for MnPS₃ the antiferromagnetic axis is collinear with the trigonal axis in agreement with the neutron-scattering results.⁸

For a two-dimensional antiferromagnet, the Néel temperature is defined as the temperature at which the slope of the susceptibility-vs-temperature curve is a maximum.¹⁴ For MnPS₃ the Néel temperature is 78 K. The broad maximum above the Néel temperature is due to short-range spin-spin correlation and is typical of low-dimensional magnetic systems. The susceptibility curve for MnPS₃ is very similar to that of the extensively studied¹⁵ two-dimensional antiferromagnet K₂MnF₄. The slight increase in χ_{\perp} below T_N (also seen in K₂MnF₄) arises due to contribution from spin waves.¹⁵

B. FePS₃

The magnetic susceptibility of FePS₃ as a function of temperature is shown in Fig. 3. Unlike MnPS₃, the susceptibility shows considerable anisotropy, χ_{\parallel} being nearly twice that of χ_{\perp} . The susceptibility curves are similar to that reported by Jernberg, Bjarman, and Wappling.¹⁶ The susceptibility curve for FePS₃ shows all the characteristics of two-dimensional magnetic ordering, both χ_{\parallel} and χ_{\perp} showing a broad maxima at 130 K. The Néel temperature, the temperature at which the slope of χ vs T is a maximum, is 123 K. Below the Néel temperature the behavior is as expected for an antiferromagnet, χ_{\parallel} dropping sharply with temperature while χ_{\perp} remains constant.

C. NiPS₃

The temperature variation of the magnetic susceptibility of NiPS₃ single crystals is shown in Fig. 4. The di-

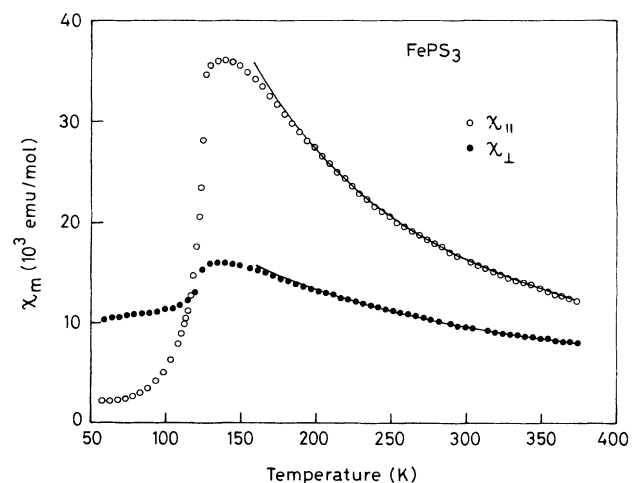


FIG. 3. Magnetic susceptibility of FePS₃ single crystals, parallel (χ_{\parallel}) and perpendicular (χ_{\perp}) to the trigonal axis, as a function of temperature. The solid lines are the least-squares fit to the anisotropic susceptibility equations; for χ_{\parallel} , $\lambda = -92.8 \text{ cm}^{-1}$, $zJ/k = -12.4 \text{ K}$ and for χ_{\perp} , $\lambda = -89.8 \text{ cm}^{-1}$, $zJ/k = 8.1 \text{ K}$.

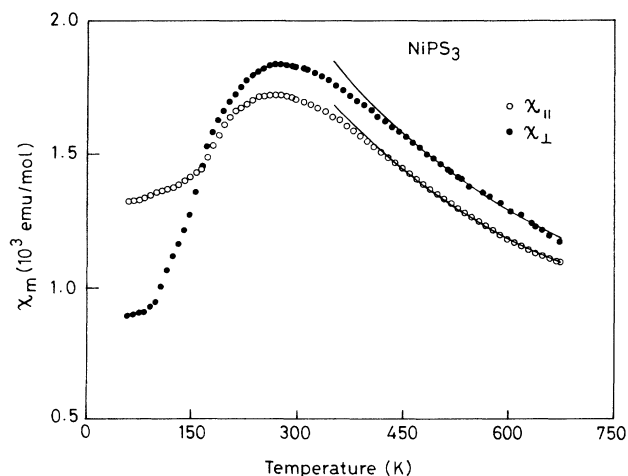


FIG. 4. Magnetic susceptibility of NiPS₃ single crystals, parallel ($\chi_{||}$) and perpendicular (χ_{\perp}) to the trigonal axis, as a function of temperature. The solid lines are the least-squares fit of the anisotropic susceptibility equations for $zJ/k = -180$ K, $D = 13$ K, and $g = 2.05$.

amagnetic and temperature-independent paramagnetic susceptibilities have been subtracted from the observed values. The temperature-independent paramagnetism (TIP) is given by $\gamma N\mu_{\beta}^2/10Dq$.¹⁷ For Ni²⁺ in an octahedral crystalline field with a ³A_{2g} singlet ground state, the constant $\gamma = 8$. The crystal-field-splitting parameter, $10Dq$, has been reported to be 8900 cm⁻¹ from optical-absorption studies.¹⁸ Substituting these values gives the TIP contribution as 0.235×10^{-3} emu/mol.

The characteristic feature of the $\chi(T)$ curve is a broad maximum with χ_{\max} at 270 K. Below this temperature the material undergoes an antiferromagnetic transition with a Néel temperature of 155 K. In contrast to MnPS₃ and FePS₃, the magnetization axis is found to be perpendicular to the trigonal axis; the spins are oriented in the *ab* plane. In the figure, $\chi_{||}$ refers to the susceptibility parallel to the trigonal axis. Since the magnetization axis is found to be lying perpendicular to this axis, below the Néel temperature, the true parallel and perpendicular susceptibilities will be in the reverse order.

V. DISCUSSION

A. Crystal-field theory

In this section we shall briefly discuss the effect of the trigonal crystal field as well as spin-orbit coupling on the susceptibilities of isolated Mn²⁺ (*d*⁵), Fe²⁺ (*d*⁶), and Ni²⁺ (*d*⁸) ions. The splittings of the ground levels of Mn²⁺, Fe²⁺, and Ni²⁺ in the weak-field limit, are shown in Fig. 5. Optical-absorption spectra¹⁸ of these compounds had shown that the weak-field limit of crystal-field theory, rather than the strong field, is more appropriate in describing the 3*d* states in these compounds.

In MnPS₃, the Mn²⁺ ion is in the high spin ⁶S ground

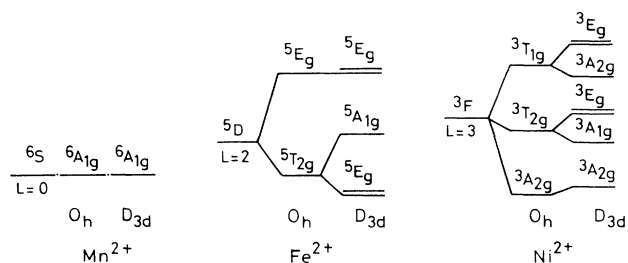


FIG. 5. The splittings of the ground levels of Mn²⁺, Fe²⁺, and Ni²⁺ by octahedral and trigonal fields.

state, which transforms to ⁶A_{1g} in the octahedral crystal-line field. The effect of spin-orbit coupling as well as the trigonal distortion are expected to be negligible for this ground state. Consequently the single-ion anisotropic term, D , is small. The reported value of D from the EPR spectra¹⁹ of Mn²⁺-doped CdPS₃ was 0.0365 cm⁻¹. As expected, the magnetic susceptibility of MnPS₃ in the paramagnetic region shows no anisotropy. The magnetic interactions may therefore be described by the Heisenberg Hamiltonian.

The trigonal distortion of the FeS₆ octahedra splits the low-energy ⁵T_{2g} states into a doublet (⁵E_g) and a singlet (⁵A_{1g}). The sign of the splitting energy determines whether the singlet or doublet is lower in energy. When Δ (trigonal splitting parameter) is negative, the orbital doublet is the ground state and vice versa. The trigonal distortion may be represented as a deviation of θ (Ref. 20) (Fig. 6), the angle between the Fe-S bond and the principal rotation axis (C_3), from the true octahedral value of 54.75°. A trigonal compression occurs when $\theta > 54.75^\circ$ and a trigonal elongation when $\theta < 54.75^\circ$.

The effect of θ in determining whether the doublet or singlet will be the ground state, is best seen for the Fe²⁺ ion in the strong-field limit. The octahedral environment splits the fivefold degenerate *d* orbitals into the triply degenerate *t*_{2g} and a doubly degenerate *e*_g orbital. Considering the C_3 axis as the axis of quantization,²¹ the *t*_{2g} orbitals are

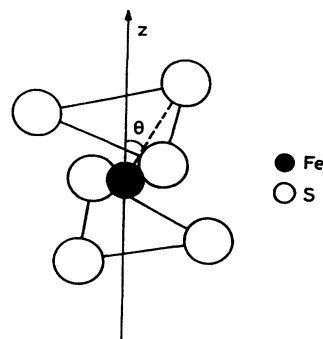


FIG. 6. Definition of the angle θ , the angle between the Fe-S bond and the C_3 axis.

$$|z^2\rangle, \\ \sqrt{\frac{2}{3}}|(x^2-y^2)\rangle - \sqrt{\frac{1}{3}}|(xz)\rangle, \\ \sqrt{\frac{2}{3}}|(xy)\rangle + \sqrt{\frac{1}{3}}|(yz)\rangle.$$

It may be seen that a trigonal elongation ($\theta < 54.75^\circ$) will destabilize the $|z^2\rangle$ with respect to the other two, so that the doublet will be lower in energy with respect to the singlet. On the other hand, trigonal compression will stabilize the $|z^2\rangle$, so that the singlet will be the ground state. Thus, one would expect the doublet to be lower in energy in FePS_3 where $\theta < \theta_{\text{oct}}$.

Additional evidence for a doublet ground state comes from the fact that a singlet ground state would give isotropic g values and would cause the spins to lie in the basal plane. The present investigation shows that the g values are anisotropic and the antiferromagnetic magnetization axis is collinear with the trigonal axis. As mentioned earlier, when the doublet is the ground state, the spin Hamiltonian [Eq. (2)] is no longer appropriate and a different procedure has to be adopted.

The magnetic property of any system depends upon the energy levels of the states populated within a given temperature range and also the levels which may mix significantly with the ground state under perturbations such as spin-orbit coupling or Zeeman effect. Since the cubic crystal field is much larger than the trigonal crystal field only the lower triplet is to be considered for analysis. The triplet level may be labeled by a fictitious angular momentum²² $l=1$ (by the isomorphism between the states of the triplet and those of p^n symmetry). The orbital angular momentum vector \mathbf{L} may now be expressed as

$$\mathbf{L} = \alpha \mathbf{l}. \quad (3)$$

$\alpha = -1$ for Fe^{2+} in a cubic crystal field. The presence of the trigonal distortion modifies the orbital wave function but α may still be considered to be close to 1 if the distortion is small.

The total Hamiltonian for the triplet state may be written as²³

$$\mathcal{H} = \Delta L_z^2 + \alpha \lambda \mathbf{l} \cdot \mathbf{S} + \mu_B (\alpha \mathbf{l} + 2\mathbf{S}) \cdot \mathbf{H}, \quad (4)$$

where $S=2$ for a high spin d^6 system. The first term corresponds to the trigonal splitting of the triplet ${}^5T_{2g}$ to the doublet (5E_g) with $L_z=1$ and the singlet (${}^5A_{1g}$), $L_z=0$. The second term gives the spin-orbit coupling where λ is the spin-orbit coupling coefficient. For Fe^{2+} (d^6), where the shell is more than half filled, λ is negative. For a free ion²⁴ Fe^{2+} , $\lambda_0 = -100 \text{ cm}^{-1}$. The last term is the Zeeman term.

The perturbed wave functions will have a considerable amount of orbital angular momentum due to the first-order splitting of the degenerate ground state in λ/Δ , and the g values are expected to be different from the spin-only values. This is in contrast to the situation when the orbital singlet is the ground state, for which the g values are isotropic and very close to the spin-only values.

The energy values obtained by diagonalization of the energy matrix²⁵ are shown in Fig. 7. The magnetic susceptibility is given in terms of g by

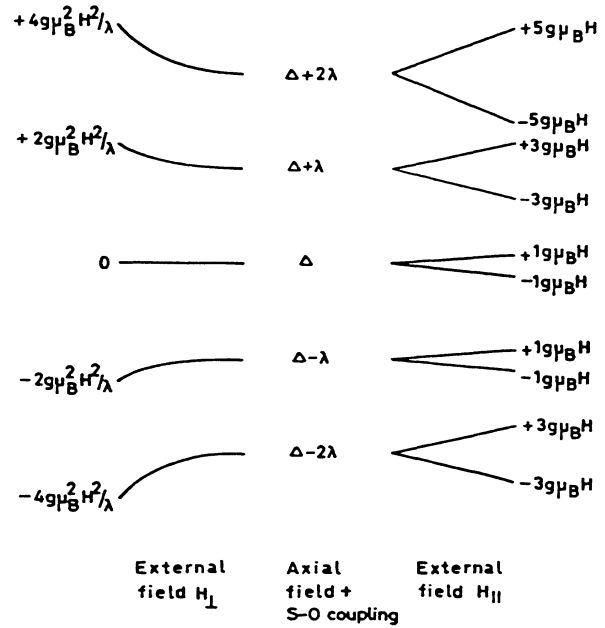


FIG. 7. Energy levels corresponding to $S=2$ for the Hamiltonian (4) in the absence of an external field ($H=0$), with the applied field parallel to the trigonal axis ($H=H_{\parallel}$) and with the field perpendicular to the trigonal axis ($H=H_{\perp}$).

$$\chi_i = N g_i^2 \mu_B^2 S(S+1) / 3kT, \quad (5)$$

where

$$g_i^2 = \frac{3(kT)^2}{S(S+1)} \frac{\partial^2}{\partial H^2} (\ln Z_i), \quad i = \parallel \text{ or } \perp \quad (6)$$

and $Z = \sum \exp(-E_j/kT)$ is the partition function, where E_j are the energies of the accessible states. The g_{\parallel} and g_{\perp} are given by

$$g_{\parallel}^2 = \frac{1}{2} \frac{25e^{-2x} + 9e^{-x} + 1 + e^x + 9e^{2x}}{e^{-2x} + e^{-x} + 1 + e^x + e^{2x}}, \quad (7)$$

$$g_{\perp}^2 = \frac{1}{2x} \frac{8(e^{2x} - e^{-2x}) + 4(e^x - e^{-x})}{e^{-2x} + e^{-x} + 1 + e^x + e^{2x}}, \quad (8)$$

where $x = \lambda/kT$ and the summation is only over the doublets.

For Ni^{2+} the ground state ${}^3A_{2g}$ (Γ_5) in a cubic field is orbitally nondegenerate and consequently one does not expect it to be affected by a trigonal distortion.²¹ The trigonal field, however, can split the first excited triplet state ${}^3T_{2g}$ (Γ_5) into a doublet and a singlet. This splitting perturbs the ground state ${}^3A_{2g}$ multiplet, indirectly via spin-orbit coupling, leading to a small zero-field splitting. Since the splitting of the cubic ground state by the trigonal distortion is an indirect effect, the splitting is likely to be very small. These splittings are shown in Fig. 8 for Ni^{2+} (d^6). From optical-absorption spectra of NiPS_3 ,¹⁸ the spin-orbit coupling constant had been found to be -280 cm^{-1} . Thus in NiPS_3 the above scenario is likely to hold.

The splitting of the $S=1$ ground-state triplet (${}^3A_{2g}$ is

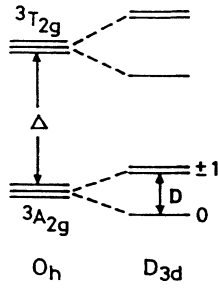


FIG. 8. Splitting of the Γ_5 states (${}^3A_{2g}$ and ${}^3T_{2g}$) for d^8 under the influence of a trigonal field. Δ is the crystal-field splitting and D , the zero-field splitting.

a orbital singlet) may be represented by the Hamiltonian,

$$\mathcal{H} = DS_z^2, \quad (9)$$

where D is the zero-field splitting. When $D > 0$ the triplet splits into a lower singlet and an upper doublet, giving $\chi_{\perp} > \chi_{\parallel}$. When $D < 0$, the doublet is the ground state, so that $\chi_{\parallel} > \chi_{\perp}$. The anisotropy of the measured susceptibility shows that in NiPS_3 , $D > 0$. When an external magnetic field is applied, these levels are further split by the Zeeman interaction, and the total Hamiltonian becomes (in the absence of exchange)

$$\mathcal{H} = DS_z^2 + g\mu_{\beta}\mathbf{S}\cdot\mathbf{H}. \quad (10)$$

Depending on the direction of the applied magnetic field, parallel or perpendicular to the axis of distortion, the energy of the states will be as shown in Fig. 9.

The magnetic susceptibility in the presence of this zero-field splitting is given by²

$$\chi_{\parallel}^0 = C \frac{2e^{-x}}{1 + 2e^{-x}}, \quad (11)$$

$$\chi_{\perp}^0 = C \frac{(2/x)(1 - e^{-x})}{1 + 2e^{-x}}, \quad (12)$$

where $x = D/kT$ and $C = Ng^2\mu_{\beta}^2/kT$.

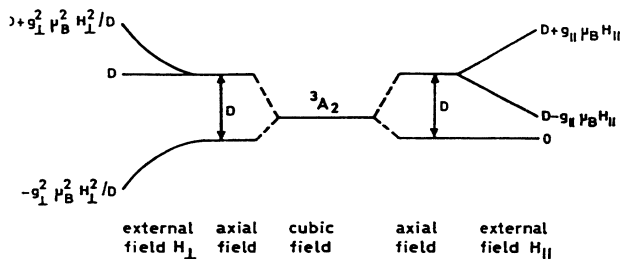


FIG. 9. Energy levels corresponding to $S = 1$ for the Hamiltonian (10) in the absence of an external field ($H = 0$), with the applied field parallel to the trigonal axis ($H = H_{\parallel}$) and with the field perpendicular to the trigonal axis ($H = H_{\perp}$).

B. Data analysis

1. MnPS_3

Above 200 K the χ_m^{-1} -vs- T curve shows a Curie-Weiss behavior. The effective magnetic moment μ_{eff} calculated from the slope is 5.97 BM, which is close to the spin-only value of 5.90 BM expected for a high spin d^5 system. The Weiss constant Θ is -160 K, indicating fairly strong antiferromagnetic interactions.

In the low-temperature antiferromagnetic state of MnPS_3 , the magnetization axis is perpendicular to the layers. The two factors that decide the axis of magnetization are the single-ion anisotropy and dipolar anisotropy. The single-ion anisotropy, as stated earlier, is negligible and even if significant, would have caused the spins to lie in the layer rather than perpendicular to it. Thus the antiferromagnetic axis is decided by the dipolar anisotropy of the ordered state. The exchange parameter J was estimated from the paramagnetic region of the experimental susceptibility within the mean-field approximation, as well as by the high-temperature series expansion.

Molecular-field theory. In the molecular-field treatment, for a two-sublattice model, the magnetic susceptibility in the paramagnetic region is given by²⁶

$$\chi_m = \frac{C}{T - C\gamma}, \quad (13)$$

where

$$C\gamma = \frac{2zJS(S+1)}{3k} = \Theta. \quad (14)$$

J is the nearest-neighbor exchange interaction and z is the number of nearest neighbors. $z = 3$ for a honeycomb lattice. The exchange integral, calculated using Eq. (14) from the experimental value of Θ (-160 K) is $J = -9.1$ K. The calculated susceptibility for $J = -9.1$ K is shown in Fig. 2.

High-temperature series expansion. The molecular-field theory gives poor agreement with experiment (Fig. 2). This is not unexpected, since it is a poor approximation in low-dimensional systems, where short-range correlations are much more important than in three-dimensional systems. The susceptibility for a two-dimensional Heisenberg antiferromagnet has been evaluated by Rushbrooke and Wood.²⁷ At sufficiently high temperatures, much above the critical temperature, the magnetic susceptibility may be expressed as a series expansion in J/kT , where J is the nearest-neighbor exchange interaction. The magnetic susceptibility for an antiferromagnet is given by

$$\chi_m = \frac{Ng^2\mu_{\beta}^2S(S+1)}{3kT} \frac{1}{1 + \sum_{i=1}^6 (-1)^i b_i (J/kT)^i}, \quad (15)$$

where μ_{β} is the Bohr magneton, S , the spin of Mn^{2+} ; J , the exchange parameter and b_i , the expansion coefficients, depend on the type of magnetic lattice. The $(-1)^i$ term is to account for the antiferromagnetic nature of the interaction. For MnPS_3 , which has a honeycomb

lattice, the constants calculated using the formula of Rushbrooke and Wood²⁷ are $b_1=17.5$, $b_2=110.833$, $b_3=304.111$, $b_4=991.828$, $b_5=9346.14$, and $b_6=264381.31$.

A least-squares fit using the above expression to the experimental data gave reasonable agreement for $J/k = -8.1$ K and $g = 2.010$. Earlier workers had obtained the value of -17.4 K (Ref. 28) and -19.2 K (Ref. 7) for J/k , by fitting to the powder susceptibility of MnPS_3 . However, there appears to be an error in the calculation of the b_i coefficients.

The least-squares-fitted curve is shown in Fig. 2. The agreement above 200 K suggests that the Heisenberg Hamiltonian is a reasonable approximation for magnetic interactions in MnPS_3 . The deviation at low temperatures may be due to (i) the range of exchange interactions being more than nearest neighbor and/or (ii) dipolar anisotropy (which decides the magnetization axis), which gives the system a weak Ising character as in MnF_2 .²⁹

2. FePS_3

The high-temperature paramagnetic susceptibility (above 200 K) in both directions, χ_{\parallel} and χ_{\perp} , obey the Curie-Weiss law. A striking feature is the large difference of the Weiss constant Θ for the two directions, although the value of μ_{eff} is comparable. The results are tabulated below.

$$\chi_{\parallel}, \mu_{\text{eff}} = 5.67 \text{ BM and } \Theta = 53 \text{ K},$$

$$\chi_{\perp}, \mu_{\text{eff}} = 5.23 \text{ BM and } \Theta = -54 \text{ K}.$$

The effective moment is larger than the spin-only value, 4.94 BM , for a high spin Fe^{2+} ion, suggesting a sizable spin-orbit contribution.

The powder susceptibility of FePS_3 has been reported by various groups with widely differing values of Θ , both positive [65 K (Ref. 30), 14 K (Ref. 31), 104 K (Ref. 7), 15 K (Ref. 8)] and negative [-15 K (Ref. 32)]. These results may be understood in the light of the present single-crystal work as originating from the preferred orientation of crystallites in the powder. When a majority of the crystallites have their basal plane preferentially oriented with respect to the magnetic field, a positive Θ would be obtained, whereas if the preferred orientation is perpendicular, a negative Θ would be obtained. Kurosawa, Saito, and Yamaguchi⁶ have estimated the exchange parameters from T_N and Θ , as obtained from powder susceptibility measurements. Such a calculation is in error because for FePS_3 , Θ is not the Weiss constant of the molecular-field approximation, but contains a contribution from antiferromagnetic exchange, as well as from the strong anisotropy.

The difference in sign of the Weiss constants is quite unusual, being positive in the parallel and negative in the perpendicular direction. It may be noted that Θ arises from contributions due to both single-ion anisotropy as well as exchange interactions. Since FePS_3 is an antiferromagnet, with the susceptibilities below T_N behaving very much as expected, the large difference in Θ values

probably originates from crystal-field effects arising due to the trigonal elongation of the FeS_6 octahedra.

In Sec. V A the expression for the susceptibility for the Fe^{2+} ion in a trigonally distorted environment was derived [Eqs. (5), (7), and (8)]. The susceptibilities so obtained are for an ensemble of noninteracting Fe^{2+} ions. Exchange interaction between the Fe^{2+} ions was accounted for by redefining the susceptibility using a simplified molecular-field approximation.²⁶ For weak applied fields and temperatures where no spontaneous ordering occurs, the susceptibility is given by

$$\chi_i = \frac{\chi_i^0}{1 - (2zJ/Ng_i^2\mu_{\beta}^2)\chi_i^0}, \quad i = \parallel \text{ or } \perp \quad (16)$$

where g_i (g_{\parallel} and g_{\perp}) are given by Eqs. (7) and (8) and χ_i^0 by Eq. (5). The experimental data were fitted using the above equation for both χ_{\parallel} and χ_{\perp} . The best fit was obtained for

$$\chi_{\parallel}, \lambda = -92.8 \text{ cm}^{-1} \text{ and } zJ/k = -12.4 \text{ K},$$

$$\chi_{\perp}, \lambda = -89.8 \text{ cm}^{-1} \text{ and } zJ/k = 8.1 \text{ K}.$$

The susceptibilities calculated with the above values of λ and zJ/k are shown in Fig. 3 as solid lines. The difference in the sign of the molecular field, $2zJS(S+1)/3k$, for the two directions is a reflection of the fact that the magnetic structure of a layer of FePS_3 consists of ferromagnetic chains coupled antiferromagnetically with the neighboring chains perpendicular to the layers.

A positive feature of the fit is that the spin-orbit coupling constants for the two independent directions are found to be nearly identical, $\sim -90 \text{ cm}^{-1}$. The spin-orbit coupling constant λ is close to the free ion value λ_0 . The reduction of λ from the free ion value is a measure of the covalency of the system. For FePS_3 $\lambda/\lambda_0 = 0.9$ implies a fairly ionic environment of the Fe^{2+} ion. A similar conclusion had been obtained from a study of the optical-absorption spectra¹⁸ of FePS_3 . An analysis of the spectra had given values of the Racah interelectron repulsion parameters, B and C , close to that of the free ion value, showing that Fe^{2+} is in an ionic environment.

Substituting for λ in Eqs. (7) and (8) gives highly anisotropic g values. The role of g in deciding the dimensionality of the magnetic interactions is best described by reformulating Eq. (1) for FePS_3 in an effective spin, $S = \frac{1}{2}$, formalism. The true spin S may be replaced by an effective spin $S' = \frac{1}{2}$ where $S_i = \frac{1}{2}(g_S S'_i)$. In this formulation Eq. (1) now becomes

$$\mathcal{H} = -2 \sum [J'_{\perp}(g'_{S\perp}/2)^2(S'_{ix}S'_{jx} + S'_{iy}S'_{jy}) + J'_{\parallel}(g'_{S\parallel}/2)^2S'_{iz}S'_{jz}]. \quad (17)$$

The original form may be recovered by substituting an effective exchange constant, $J'_i = (g_i/2)^2 J$, in the above equation. It may be seen that $J'_{\parallel}/J'_{\perp} = (g_{\parallel}^2/g_{\perp}^2)J_{\parallel}/J_{\perp}$. For FePS_3 even at room temperature $g_{\parallel}^2/g_{\perp}^2 > 2$, with the ratio increasing with decreasing temperature. Thus FePS_3 may be effectively treated by the Ising model, the

anisotropy of the magnetic interactions arising from the anisotropy in g . The g anisotropy also decides that in the antiferromagnetic state the magnetization axis would be parallel to the trigonal axis.

3. NiPS₃

The susceptibility of NiPS₃ at high temperatures shows weak anisotropy with $\chi_{\perp} > \chi_{\parallel}$ (the susceptibilities are with respect to the trigonal axis). A Curie-Weiss fit to the susceptibility above 400 K gave $\mu_{\text{eff}\parallel} = 2.83BM$ and $\mu_{\text{eff}\perp} = 2.97BM$, which are close to the spin-only value for an Ni²⁺ ion. The corresponding Θ values are -241 and -254 K, respectively. Earlier workers^{7,31} had reported a μ_{eff} value of $3.7BM$ from the powder susceptibility of NiPS₃. However, their calculations were done on susceptibilities which were not corrected for TIP. The present data also gave similar values for μ_{eff} when the TIP contributions were not included.

The anisotropy in the susceptibilities is a consequence of the zero-field splitting of the ³A_{2g} ground state of Ni²⁺ by the trigonal distortion. The fact that $\chi_{\perp} > \chi_{\parallel}$ directly implies a splitting of the ground-state triplet into a lower singlet and an upper doublet. The weak anisotropy is a consequence of the fact that the splitting of the ³A_{2g} state by the trigonal field is an indirect effect, arising from the spin-orbit coupling of the ³A_{2g} state with the higher-lying ³T_{2g} state, whose degeneracy is lifted by the trigonal field.

Since the zero-field splitting D is small, Eqs. (11) and (12) may be further simplified to

$$\chi_{\parallel}^0 = C \frac{2(1-D/kT)}{1+2(1-D/kT)}, \quad (18)$$

$$\chi_{\perp}^0 = C \frac{2}{1+2(1-D/kT)}. \quad (19)$$

The above equations were further modified to account for exchange interactions. This was done in the molecular-field approximation by using Eq. (16). Solving the exchange modified susceptibility equations gave a value of zJ/k as -180 K.

A least-squares fit of the susceptibility expressions to the experimental data above 400 K was performed using the above value of J and by keeping D and g as input variables. In doing so it was assumed that the exchange interactions are isotropic, so that the value of zJ/k can be taken as -180 K for both parallel and perpendicular directions. The fittings gave a value of $D/k \sim 13$ K and $g = 2.05$. The g value obtained is much less than what is expected for Ni²⁺ in a trigonal field. The g value may be calculated from the expression $g = 2.00(1 - 8\lambda/10Dg)$. For $\lambda = -280$ cm⁻¹, the spin-orbit coupling constant for NiPS₃ obtained from a weak-field analysis of the optical-absorption spectra,¹⁸ g is calculated as 2.25.

The calculated susceptibility curves in the parallel and perpendicular directions using the values of J , D , and g are shown in Fig. 4 as full lines. The reason for the low- g value may be the fact that short-range correlations are

important even at temperatures much higher than $2T_N$, so that the mean-field treatment is a poor approximation and the susceptibility equations are not truly valid. The small but positive D would, in the absence of any other anisotropic interactions, cause the spins to be aligned in the basal plane (perpendicular to the trigonal axis).

By using arguments similar to those used for FePS₃, the magnetic Hamiltonian may be expressed using an effective constant, J' . For NiPS₃, $J'_{\perp} > J'_{\parallel}$ and the magnetic interactions are best described by the anisotropic Heisenberg Hamiltonian. The positive value of the zero-field splitting is also instrumental in determining the magnetization axis. It may be seen from Fig. 4 that below the Néel temperature, χ_{\perp} drops rapidly, with χ_{\parallel} remaining essentially constant, implying that in the antiferromagnetically ordered state the spins are aligned in the basal plane perpendicular to the trigonal axis.

VI. CONCLUSIONS

The magnetic behavior of MnPS₃, FePS₃, and NiPS₃ reveals the critical role of the trigonal distortion in deciding the nature and symmetry of the magnetic interactions. Although all three compounds are isostructural, with the transition-metal ion in the high spin state, the effects of trigonal distortion are quite different. In MnPS₃, where the effect is negligible, it leads to symmetric Heisenberg interactions. In FePS₃, the contribution of the trigonal distortion as well as the spin-orbit coupling gives rise to highly anisotropic g values, which in turn imply highly anisotropic magnetic interactions. The anisotropy is large ($g_{\parallel}^2 > g_{\perp}^2$) so that FePS₃ is best described by the Ising Hamiltonian. In contrast, the combination of trigonal distortion and spin-orbit coupling in NiPS₃ causes the spins to lie in the basal plane, so that the system is best represented by the anisotropic Heisenberg Hamiltonian.

In FePS₃ and NiPS₃, the magnetization axis of the antiferromagnet is determined by the single-ion anisotropy, whereas in MnPS₃, where such terms are negligible, the magnetization axis is probably determined by the magnetic dipolar anisotropy of the ordered state.

The transition-metal thiophosphates MPS_3 ($M = \text{Mn}, \text{Fe}, \text{and Ni}$) form a unique class of compounds in which the spin dimensionality may be controlled by the choice of the transition-metal ion. Since the thiophosphates are isostructural, solid solutions between members of the group are easily formed and provide a convenient way of studying the problem of competing spin anisotropies. Magnetic studies of solid solutions of the transition-metal thiophosphates will be reported in a subsequent publication.

ACKNOWLEDGMENTS

The authors thank the Department of Science and Technology for financial assistance. One of us (P.A.J.) is grateful to CSIR, India for partial support.

- ¹L. De Jongh and A. R. Miedema, *Adv. Phys.* **23**, 1 (1974).
- ²R. L. Carlin, *Magnetochemistry* (Springer-Verlag, Berlin, 1974).
- ³*Magnetostructural Correlations in Exchange Coupled Systems*, edited by R. D. Willet *et al.* (Riedel, Dordrecht, 1985).
- ⁴R. Brec, *Solid State Ionics* **22**, 3 (1986).
- ⁵E. Koster and J. Steger, *J. Solid State Chem.* **3**, 273 (1971).
- ⁶W. Klingen, G. Eulenberger, and H. Hahn *Z. Anorg. Allg. Chem.* **401**, 97 (1973); G. Ouvrard, R. Brec, and J. Rouxel *Mat. Res. Bull.* **20**, 1181 (1985).
- ⁷G. Le Flem, R. Brec, G. Ouvrard, A. Louisy, and P. Segransen, *J. Phys. Chem. Solids* **43**, 455 (1982).
- ⁸K. Kurosawa, S. Saito, and Y. Yamaguchi, *J. Phys. Soc. Jpn.* **52**, 3919 (1983).
- ⁹P. A. Joy, Ph.D. thesis, IISc., Bangalore, India, 1990 (unpublished).
- ¹⁰*Intercalation Chemistry*, edited by M. S. Whittingham and A. J. Jacobson (Academic, New York, 1982); *Intercalated Layered Materials*, edited by F. Levy (Riedel, Dordrecht, 1979).
- ¹¹R. Clement, O. Garnier, and J. Jegoudez, *Inorg. Chem.* **25**, 1404 (1986); G. A. Fatseas, M. Evain, G. Ouvrard, and R. Brec, *Phys. Rev. B* **35**, 3082 (1987).
- ¹²J. B. Goodenough, *Magnetism and the Chemical Bond* (Wiley Interscience, New York, 1963).
- ¹³R. Nitsche and P. Wild, *Mat. Res. Bull.* **5**, 419 (1970).
- ¹⁴M. E. Fisher, *Philos. Mag.* **7**, 1731 (1962).
- ¹⁵D. J. Breed, *Physica* **37**, 35 (1967).
- ¹⁶P. Jernberg, S. Bjarman, and W. Wappling, *J. Magn. Magn. Mater.* **46**, 178 (1984).
- ¹⁷F. E. Mabbs and D. J. Machin, *Magnetism and Transition Metal Complexes* (Chapman and Hall, London, 1973).
- ¹⁸P. A. Joy and S. Vasudevan, this issue, *Phys. Rev. B* **46**, 5134 (1992).
- ¹⁹D. A. Cleary, A. H. Francis, and E. Lifshitz, *Chem. Phys.* **106**, 123 (1986).
- ²⁰M. Gerloch, J. Lewis, G. G. Philips and P. N. Queded, *J. Chem. Soc. A* p. 1941 (1970).
- ²¹C. J. Ballhausen, *Introduction to Ligand Field Theory* (McGraw-Hill, New York, 1962).
- ²²A. Abragam and B. Bleaney, *EPR of Transition Ions* (Clarendon, Oxford, 1970).
- ²³H. Nozaki, M. Umehara, Y. Ishizawa, and M. Sacki, *J. Phys. Chem. Solids* **39**, 851 (1978).
- ²⁴J. S. Griffith, *The Theory of Transition Metal Ions* (Cambridge University Press, Cambridge, 1961), p. 437.
- ²⁵S. S. P. Parkin and R. H. Friend, *Philos. Mag.* **41**, 65 (1980).
- ²⁶J. S. Smart, *Effective Field Theories of Magnetism* (Saunders, Philadelphia, 1986).
- ²⁷G. S. Rushbrooke, and P. J. Wood, *Mol. Phys.* **1**, 257 (1958).
- ²⁸R. Clement, J. J. Girerd, and I. M. Badarau, *Inorg. Chem.* **19**, 2852 (1980).
- ²⁹E. E. Bragg and M. S. Seehra, *Phys. Rev. B* **7**, 4197 (1973); R. A. Cowley and W. J. C. Buyers, *J. Phys. C* **15**, L1209 (1982).
- ³⁰R. Brec, D. M. Schleich, G. Ouvrard, A. Louisy, and J. Rouxel, *Inorg. Chem.* **18**, 1814 (1979).
- ³¹B. E. Taylor, J. Steger, and A. Wild, *J. Solid State Chem.* **7**, 461 (1973).
- ³²K. Okuda, K. Kurosawa, and S. Saito, in *High Field Magnetism*, edited by M. Date (North-Holland, Amsterdam, 1983), p. 55.